GIS Based Landslide Susceptibility Mapping using a Fuzzy Logic Approach: A Case Study from Ghurmi-Dhad Khola Area, Eastern Nepal

4 authors, including:

P. Kayastha
Vrije Universiteit Brussel
16 PUBLICATIONS   1,005 CITATIONS

SEE PROFILE

Subeg Bijukchhen
Khwopa Engineering College
21 PUBLICATIONS   308 CITATIONS

SEE PROFILE

Megh Raj Dhital
Tri-Chandra Multiple Campus, Ghantaghar
95 PUBLICATIONS   2,544 CITATIONS

SEE PROFILE

Some of the authors of this publication are also working on these related projects:

Landslide susceptibility assessment in the Kankai watershed, Nepal View project

Landslide susceptibility assessment the Tinau watershed, Nepal View project

GIS Based Landslide Susceptibility Mapping using a Fuzzy Logic Approach: A Case Study from Ghurmi-Dhad Khola Area, Eastern Nepal

Prabin Kayastha[1,2], Subeg Man Bijukchhen[3], Megh Raj Dhital[2,3] and Florimond De Smedt[1]

[1]Department of Hydrology and Hydraulic Engineering, Vrije Universiteit Brussel, Pleinlaan 2, 1050 Brussels, Belgium.
[2]Mountain Risk Engineering Unit, Tribhuvan University, Kirtipur, Kathmandu, Nepal.
[3]Central Department of Geology, Tribhuvan University, Kirtipur, Kathmandu, Nepal.
Email: pkayasth@vub.ac.be

Abstract: Landslides cause extensive loss of life and property in the Nepal Himalaya. Since the late 1980s, different mathematical models have been developed and applied for landslide susceptibility mapping and hazard assessment in Nepal. The main goal of this paper is to apply fuzzy logic to landslide susceptibility mapping in the Ghurmi-Dhad Khola area, Eastern Nepal. Seven causative factors are considered: slope angle, slope aspect, distance from drainage, land use, geology, distance from faults and folds, soil and rock type. Likelihood ratios are obtained for each class of causative factors by comparison with past landslide occurrences. The ratios are normalized between zero and one to obtain fuzzy membership values. Further, different fuzzy operators are applied to generate landslide susceptibility maps. Comparison with the landslide inventory map reveals that the fuzzy gamma operator with a γ-value of 0.60 yields the best prediction accuracy. Consequently, this operator is used to produce the final landslide susceptibility zonation map.

Keywords: Landslide, GIS, Susceptibility, Fuzzy operator, Nepal.

INTRODUCTION

Nepal being a country with rugged and fragile mountain topography is prone to a number of natural disasters like landslides, floods, earthquakes, droughts, avalanches and glacial lake outburst floods. Landslides in Nepal often occur during or after heavy monsoon rainfall resulting in the loss of life and damage to the natural and built environment. This is further aggravated by anthropogenic factors such as deforestation, haphazard migration and settlement, unsound agricultural practices and unplanned developmental works (Upreti and Dhital, 1996; Kayastha et al., 2010).

Various researchers have carried out systematic study of landslides including inventory mapping, susceptibility mapping, hazard mapping and risk assessment in different parts of the world in the last two to three decades (e.g. Aleotti and Chowdhury, 1999; Guzzetti et al., 1999; Dubey et al., 2005; Lee et al., 2012). However, in Nepal, very few have attempted to carry out systematic studies on landslides (Dhital, 2005a). As Nepal lies in a moderate to high landslide

hazard zone (Nadim et al., 2006), the present study intends to investigate the state of landslide occurrences and delineate the landslide susceptible zones in the Ghurmi-Dhad Khola area in Eastern Nepal. Various methodologies have been applied for landslide susceptibility and hazard evaluation in the Himalaya, including heuristic approaches based on expert opinion or experience (Deoja et al., 1991; Thapa and Dhital, 2000; Kayastha et al., 2010; Bijukchhen et al., 2012), statistical techniques (Dhakal et al., 1999; Dahal et al., 2008; Pantha et al., 2010; Poudyal et al., 2010; Kayastha et al., 2010; Ghimire, 2011; Bijukchhen et al., 2012; Kayastha et al., 2012) and deterministic techniques (Joshi et al., 2000; Acharya et al., 2006; Sharma and Shakya, 2008; Ray and De Smedt, 2009; Kayastha and De Smedt, 2009; Singh et al., 2012).

Another technique to derive landslide susceptibility maps is provided by the fuzzy set theory (Zadeh, 1965) as discussed by An et al. (1991) and Bonham-Carter (1994). Some researchers have applied the fuzzy logic approach for assessing landslide susceptibility, hazard and risk

mapping in the Indian Himalaya region, such as Kanungo et al. (2006; 2008; 2009) in the Darjeeling Himalaya region and Champati ray et al. (2007) in the Garhwal Himalaya region. In this study, the fuzzy logic approach will be applied for the Ghurmi-Dhad Khola area in Eastern Nepal. The objectives of this study are: (i) prepare a landslide inventory map and maps of causative factors, (ii) employ fuzzy logic to assess the impact of each factor on landsliding, (iii) apply fuzzy operators for combining all fuzzy causative factor information to derive a landslide susceptibility map of the study area, (iv) determine the most successful fuzzy logic operator to obtain the optimum landslide susceptibility map, and (v) assess and validate the accuracy of the obtained landslide susceptibility map.

STUDY AREA

The study area lies between latitudes 27°08'45" to 27°15'00" N and longitudes 86°22'30" to 86°30'00" E (Fig.1) in the Sagarmatha zone, Eastern Nepal. It covers a large part of the Okhaldhunga district and small parts of the Sindhuli as well as the Udaypur and Khotang districts, but the study mainly focuses on the Ghurmi-Dhad Khola area of the Okhaldhunga district.
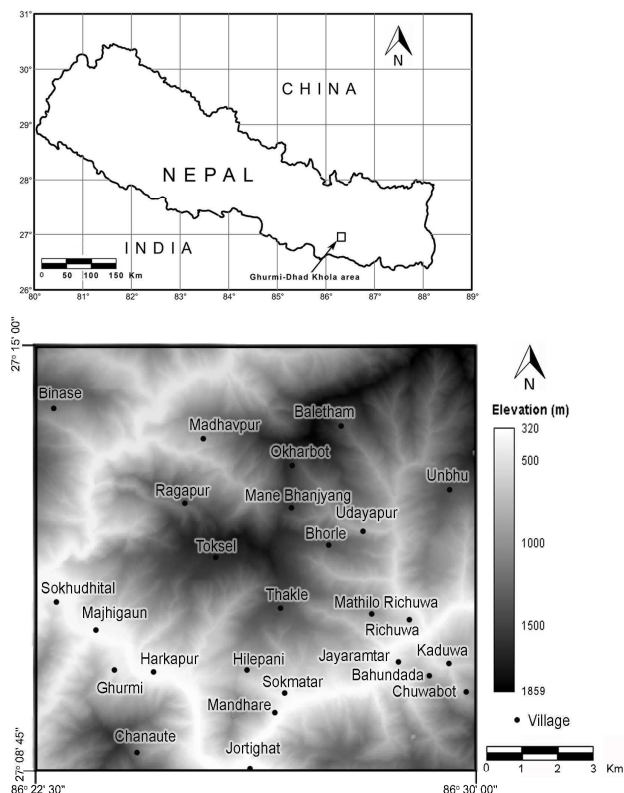
Fig.1. Location of the study area: Ghurmi-Dhad Khola area,
Eastern Nepal with Digital Elevation Model (DEM).

Climate

The climate of any area is governed by altitude and physiographic characteristics. The study area experiences a sub-tropical to temperate climate. As the altitude of the area varies from 300 m to 1859 m, variability in climate is not uncommon. The temperature ranges from 5° to 35°C, with hot summers and mild winters in the river basins and warm summers and cold winters in the higher altitudes. The average annual precipitation of the area is 1080 mm. About 80% of all precipitation occurs in the monsoon from June to the end of September. Rain intensities vary throughout the area, with a maximum intensity of rainfall occurring on the south-facing slopes.

Topography and Drainage

The study area consists of an uneven hilly terrain exhibiting rugged topography with diversified landforms. The altitude varies from 320 m at Jortighat to maximum 1859 m at Baletham (Fig.1). The drainage pattern of the study area is essentially dendritic (Fig.2). The most prominent rivers are the Sunkoshi river and the Dudhkoshi river. Both are snow-fed, perennial rivers; the former flows into the study area from the northwest and the latter from the northeast. Other rivers in the study area are the Malung Khola, Dhad Khola, Bahadur Khola, Bhadare Khola, Ramdu Khola, Odu Khola, Dothe Khola, Thare Khola and Dhuseni Khola, all tributaries of the main two rivers. Besides, there are numerous small streams feeding these tributaries.

GEOLOGY OF THE STUDY AREA

General descriptions of the regional geology have been given by Isida and Ohta (1973) and Goscombe et al. (2006). The geological map of the study area has been prepared by Gyawali and Bijukchhen (2011). The study area can be broadly separated into two units, i.e. the Lesser Himalayan sequence and the Higher Himalayan crystallines, which are separated by the Main Central Thrust (MCT). The Lesser Himalayan sequence consists of metasedimentary to low grade metamorphic rocks and can be divided into four geological formations, i.e. Para Khola Formation, Halesi dolomite, Madhavpur slates and Harkapur Formation. The Higher Himalayan crystallines consist of high-grade metamorphic rocks like schists, gneiss and quartzites (Table 1). All units are shown on the geological map of the area (Fig.3).

Para Khola Formation

The Para Khola Formation is named after the Para Khola

Fig.2. Drainage map of the study area with observed landslides.

where it is well exposed. The unit extends north from the Dhad Khola and Dhuseni Khola and consists of red-purple quartzite, sandstone and red-purple and green mottled shale with amphibolites. The thickness of the formation is more than 1000 m. The formation rests upon the younger Madhavpur slates above a thrust passing along the Dhad Khola (Dhad Khola Thrust).

Madhavpur Slates

The Madhavpur slates are named after Madhavpur village where they are well exposed. This unit predominately consists of dark grey to black graphitic slates, though light to dark grey carbonate bands are also not rare. The characteristic feature of the formation, the dark colour of the slates, can be seen in the fresh outcrops along the river or in the road section, but is rather difficult to observe in the weathered exposures as the apparent colour is much lighter. This formation is separated from the older Para Khola Formation by the Dhad Khola Thrust in the north, and gradually grades into the younger Harkapur Formation in the south, except for a sharp thrust contact (north of Kaduwa village) in the southeast part of the study area. This unit is well exposed around Koltar, Baletham, Madhavpur, Ragapur, Okharbot and Richuwa.

Harkapur Formation

The formation is well exposed around Harkapur village

and is characterised by a mixed lithology of greenish-grey calcareous phyllites, slates, siliceous dolomites, and light-grey to pink quartzite and amphibolites. It is generally more intensely deformed at the upper or southern part than in the lower part due to the movement related to the MCT. The rocks of this formation can also be seen at Toksel, Manebhanjyang, Bhorle, Kaduwa, Jayaramtar and Hilepani. Separated from older rocks of the Madhavpur slates by a transitional contact, the Harkapur Formation is separated by the MCT from the Higher Himalayan rocks and by another thrust from the Halesi dolomite.

Halesi Dolomite

This irregular band has been traced from Halesi in the Khotang district (Dhital, 2005b) to Kaduwa in the study area. Hence it is named as the Halesi dolomite. Since this unit was carried all the way from the east by the movement of the MCT, it is separated by the MCT itself from the Higher Himalayan Crystalline rocks and by another thrust from the Harkapur Formation.

Higher Himalayan Crystallines

The Higher Himalaya Crystallines lie discordantly over the Lesser Himalayan sequence, and consist of psammitic schist, pelitic schist, banded gneiss, augen gneiss, granitic gneiss, interfingering granite intrusions and a few bands of white quartzite. The Higher Himalayan Cystallines are

Table 1. Stratigraphy of the Ghurmi-Dhad Khola area, Eastern Nepal, modified from Gyawali and Bijukchhen (2011)

Rock Units	Formation	Main Lithology	Thickness
Higher Himalayan Unit	Higher Himalayan Crystallines	Psammatic schist, pelitic schist, banded gneiss, augen gneiss, granitic gneiss, interfingering granite intrusions and quartzite	>1,800 m
	- Main Central Thrust (MCT) -		
Lesser Himalayan Sequence	Harkapur Formation	Greenish-grey calcareous phyllite, slates, siliceous dolomite, light-grey to pink quartzite and amphibolites	>1,200 m
	Madhavpur Slates	Dark grey to black graphitic slate, with light to dark grey carbonate bands	>1,300 m
	Halesi Dolomite	Grey dolomite	>200 m
	Para Khola Formation	Red-purple quartzite, sandstone, red-purple and green mottled shale with amphibolites	>1,000 m

distributed around Mandhare, Jortighat, Hilepani, Ghurmi and Sokhudhital villages.

Geological Structures

The Main Central Thrust (MCT) and the Dhad Khola Thrust (DKT) are the dominant structures of the study area. The MCT juxtaposes the crystalline rocks of the Higher Himalaya over the metasedimentary rocks of the Lesser Himalaya (Acharya, 2008). Since the study area is in the southern part of the Okhaldhunga window, the MCT separates the south lying Higher Himalayan crystallines from the north lying Lesser Himalayan sequence. The E–W

trending and north-dipping Dhad Khola Thrust separates the older Para Khola Formation and younger Madhavpur slates in the northern part of the study area. The thrust can be delineated based on the contrasting lithology in its hanging wall and footwall side. The folds observed are deformed, but there is no shear or crushed zone.

A thrust in the southeast of the study separates the Madhavpur slates and the Harkapur Formation. Also the Halesi dolomite is separated from the Harkapur Formation by a south-dipping thrust more or less parallel to the MCT.

Some anticlines and one syncline are observed in the area. An E–W trending syncline in the Harkapur Formation

Fig.3. Geological map of the study area (modified from Gyawali and Bijukchhen, 2011).

is observed in the east passing through Bhorle village, but its extension towards the west is not observed. In the north part of the area, a NE–SW trending anticline is observed in the Madhavpur Slates near Simlebesi village, and another anticline north of Baletham village, which joins the DKT. Another anticline is observed just south of the syncline in the Madhavpur slates near Richuwa village. This anticline has a NW–SE trend and is overlain by the thrust separating the Madhavpur slates and Harkapur Formation.

Several mesoscopic and small-scale structures like folds, foliations, beddings, quartz veins and drag folds are common in the area. The rock units are highly folded and deformed in most part of the study area. The phyllites of the Harkapur Formation are most deformed. The slates of Madhavpur Formation also contain deformed and disrupted quartz veins at some locations.

DATA PREPARATION

For landslide susceptibility mapping, a number of thematic data on causative factors were identified. These include geology, distance from folds and faults, distance from drainage, rock and soil type, slope angle, slope aspect and land use. Topographic maps and aerial photographs provided by the Department of Survey, Government of Nepal were considered as basic data sources for generating some of these layers. On the other hand, field surveys were carried out from January to March 2011 for further data collection and geological map preparation. A landslide inventory map was also prepared in the field in conjunction with the analysis of available topographic map produced by the Department of Survey, 1995 and Google Earth images of 2002. These data sources were used to generate various thematic layers using GIS software like ILWIS 3.5, ArcGIS 9.3 and IDRISI. A brief description of these thematic layers is given below.

Landslide Inventory Map

To determine landslide hazard and predict future landslide occurrences, an understanding of the conditions and processes controlling landslides is required (Long, 2008). The landslide distribution map helps in understanding the factors and conditions controlling the landslides and is used as a basis for landslide susceptibility zonation. Preparation of a landslide distribution or inventory map is the most important and initial step for landslide susceptibility analysis. The existing landslides are taken into consideration for predicting and evaluating susceptible areas, as future landslides are likely to occur in the same geological, hydrological and geomorphic conditions as those in the past.

Three main approaches were undertaken for the preparation of the map: study of topography, interpretation of Google Earth images and fieldwork. The landslides marked on the topographic map of the Department of Survey, 1995 were updated by the study of the Google Earth images of 2002 and verified and further updated by a series of field reconnaissance in 2011. The demarcation of the landslides on the topographic map was carried out in the field using a GPS. The three approaches were coupled to prepare a reliable landslide inventory map in the form of a polygon map (Fig.2).

The study area, being a structurally complex terrain, is prone to slope instability due to its lithological and structural characteristics. The inventory map shows landslides covering 20,688 pixels, i.e. an area of 2.069 km^2 (each pixel being 10 m x 10 m in size). A total of 77 landslides were identified and it was observed that most of the landslides are located in the southern part of the study area. The landslides are observed in clusters, the most prominent one being in the Bhadare Khola (Fig.4a). Other landslide clusters are observed around the Bhalu Khola (Fig.4b).

Geological Factor

Geology is one of the prime and important causative factors causing slope instability. The geology and geological map of the study area has already been described above. Five lithological units were identified and mapped, i.e. the Para Khola Formation, Halesi dolomite, Madhavpur slates, Harkapur Formation and Higher Himalayan Crystallines (Fig.3).

Distance from Faults and Folds

The faults and folds were retrieved from the geological map (Fig.3). The distance from faults and fold to any point was calculated using the GIS Euclidean distance tool and then sub-divided into three continuous classes: (i) < 50 m, (ii) 50–100 m, and (iii) > 100 m. It is expected that landslides occur near the faults and folds and decrease as the distance increases. But the situation in the study area differs as the majority of the landslides have occurred more than 100 m away from the major folds and faults. In this particular case, probably faults and folds are not the main governing factor for the occurrence of landslides.

Distance from Drainage

To assess the effect of drainage on landslide occurrence, the distance from drainage axes was considered. It is evident from previous studies that closeness to streams will have a major effect on landslide occurrence, as intensive gully erosion is often the main cause of mass wasting. The

Table 2. Spatial relationships between each factor class and observed landslides, and resulting likelihood ratio and fuzzy membership values

Data layers	No. of pixels in domain	Percentage of domain	No. of land-slide pixels	Percentage of landslide	Likelihood ratio	Fuzzy membership value
Slope aspect						
North (N)	169,732	12.01	1,803	8.72	0.73	0.51
North-East (NE)	147,814	10.46	724	3.50	0.33	0.23
East (E)	147,667	10.45	1,076	5.20	0.50	0.35
South-East (SE)	186,215	13.18	3,470	16.77	1.27	0.89
South (S)	245,179	17.35	3,961	19.15	1.10	0.77
South-West (SW)	188,198	13.32	3,627	17.53	1.32	0.93
West (W)	161,806	11.45	3,372	16.30	1.42	1.00
North-West (NW)	165,777	11.73	2,653	12.82	1.09	0.77
Flat	445	0.03	2	0.01	0.31	0.22
Slope angle						
0^0–15^0	111,764	7.91	251	1.21	0.15	0.10
15^0–25^0	249,295	17.65	1,449	7.00	0.40	0.27
25^0–35^0	440,038	31.15	5,825	28.16	0.90	0.61
35^0–45^0	375,325	26.57	8,076	39.04	1.47	1.00
> 45^0	236,411	16.73	5,087	24.59	1.47	1.00
Soil rock type						
Rock	554,169	39.22	7,215	34.88	0.89	0.48
Alluvium soil	109,130	7.72	170	0.82	0.11	0.06
Colluvium soil	481,040	34.05	13,150	63.56	1.87	1.00
Residual soil-shallow	255,620	18.09	153	0.74	0.04	0.02
Residual soil-thick	12,874	0.91	0	0.00	0.00	0.00
Distance from drainage						
< 25m	313,404	22.18	8,079	39.05	1.76	1.00
25–50 m	243,702	17.25	4,818	23.29	1.35	0.77
50–100 m	453,311	32.09	5,824	28.15	0.88	0.50
> 100 m	402,416	28.48	1,967	9.51	0.33	0.19
Geology						
Parakhola Formation	45,355	3.21	71	0.34	0.11	0.03
Halesi Dolomite	2,751	0.19	167	0.81	4.15	1.00
Madhavpur Slates	575,997	40.77	5,662	27.37	0.67	0.16
Harkapur Formation	447,888	31.70	9,711	46.94	1.48	0.36
Higher Himalayan Unit	340,842	24.12	5,077	24.54	1.02	0.25
Land cover						
Cultivated and built-up area	642,001	45.44	3,926	18.98	0.42	0.19
Forest	644,477	45.62	14,550	70.33	1.54	0.68
Grass land	58,884	4.17	1,392	6.73	1.61	0.72
Bush	22,898	1.62	756	3.65	2.25	1.00
Sandy area	28,212	2.00	64	0.31	0.15	0.07
Water body	16,093	1.14	0	0.00	0.00	0.00
Barren land	268	0.02	0	0.00	0.00	0.00
Distance from faults and folds						
< 50 m	43,127	3.05	535	2.59	0.85	0.84
50–100 m	45,869	3.25	514	2.48	0.77	0.76
> 100 m	1,323,837	93.70	19,639	94.93	1.01	1.00
Total	**1,412,833**	**100**	**20,688**	**100**		

distance from drainage was calculated by the GIS Euclidean distance tool and the resultant values were reclassified into four classes: (i) < 25 m, (ii) 25–50 m, (iii) 50–100 m, and (iv) > 100 m. It has been observed in the field that the majority of the landslides occur in an area less than 50 m from drainage axes.

Rock and Soil Types

Rock and soil characteristics also play an important role in causing surface instability. Strength of rock, strength and depth of soil, etc. often have a strong influence on mass movements. A rock-soil type map of the area was prepared based on fieldwork showing different classes such as:

Fig.4. Panoramic view of some landslides: **(a)** the Bhadare Khola rockfall and **(b)** the landslide on the right bank of the Bhalu Khola (the arrow indicates the main scarp).

(i) rock, (ii) alluvium soil, (iii) colluvium soil, (iv) shallow residual soil (thickness less than 5 m), and (v) thick residual soil (thickness more than 5 m) (Fig.5). Due to the absence

of rock strength tests, rock types were not differentiated according to their strength.

Topographic Factors

A Digital Elevation Model (DEM) of the study area (Fig.1) with 10 m ×10 m cell size was prepared on the basis of polyline elevation contours with intervals of 20 m. The digital contours were obtained from the Department of Survey, Government of Nepal. From this DEM, geomorphological thematic data layers of slope angle and slope aspect were prepared. Slope angle is considered as a triggering factor for mass wasting because of the action of gravity. Generally, steep slopes are more prone to sliding than gentle slopes as the friction angle of the material and the earth's gravity come into play. The slope angle of the present study area was categorised into five classes: (i) < 15°, (ii) 15–25°, (iii) 25–35°, (iv) 35–45°, and (v) > 45°. The direction in which the slope faces is the slope aspect. Generally, mass movement hazard is more likely to affect slopes that face towards the sunlight and downpours than slopes in shadow zones. The slope aspect was grouped into nine classes: North (N), North-East (NE), East (E), South-East (SE), South (S), South-West (SW), West (W), North-West (NW) and flat.

Land use

Land use or land cover also affects the occurrence of
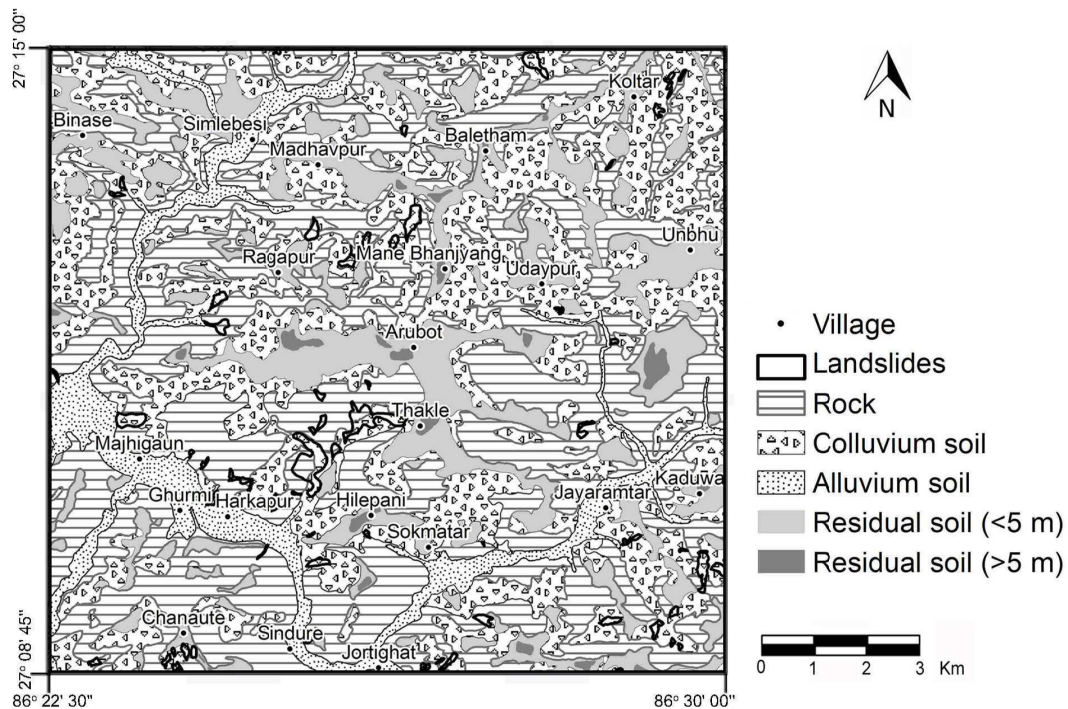
Fig.5. Rock and soil distribution map of the study area.
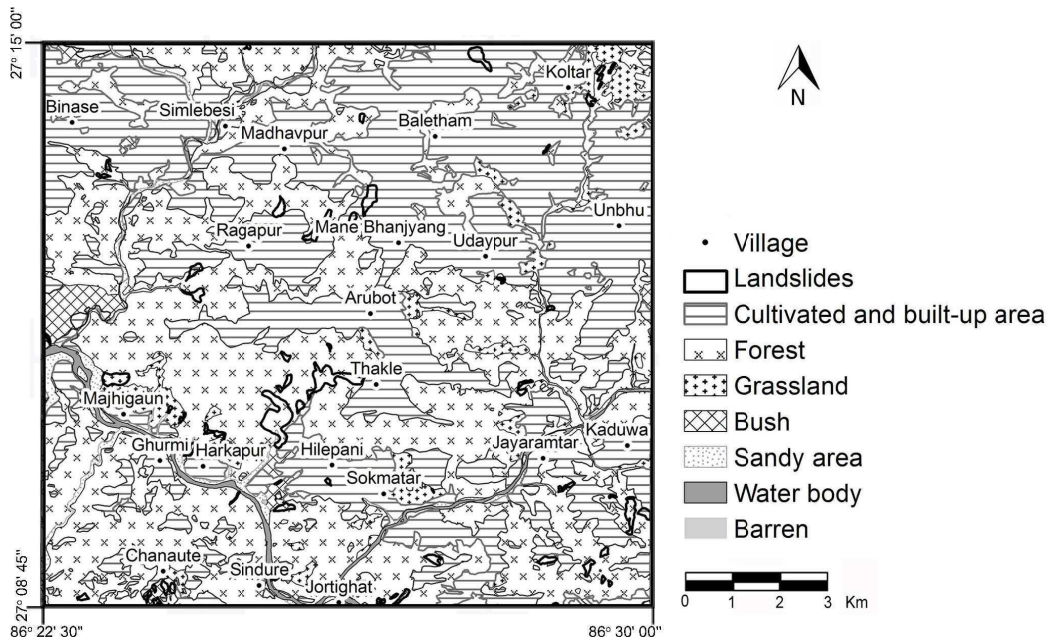
Fig.6. Land cover map of the study area.

landslides. The land cover map of the study area was provided by the Department of Survey, Government of Nepal, and verified during fieldwork. Various types of land cover (Fig.6) are found in the study area such as cultivated and built-up area, forest, grassland, bush, sandy area, water body and barren land.

METHODOLOGY

Zadeh (1965) introduced the fuzzy set theory to analyse mathematically non-discrete natural processes or phenomena. A fuzzy set is a class of objects with a continuum of grades of membership, characterized by a membership function which assigns to each object a grade of membership ranging between zero and one (Zimmermann, 1996). If X is a space of objects with a generic element of X denoted by *x*, then X = {*x*}. The fuzzy set A in X is characterized by a membership function $\mu_A(x)$, which associates with each object in X a real number in the interval [0,1], where the value of $\mu_A(x)$ represents the "grade of membership" of *x* in A. Hence, the fuzzy set theory uses the idea of a membership function to expresses the degree of membership with respect to some attribute of interest (Zadeh, 1965).

In landslide susceptibility mapping, spatial objects on a map are considered as members of a set (Tangestani, 2004; Lee, 2007). Usually, to quantify the occurrence of landslides in a certain lithological unit, the number of observed landslide occurrences in a certain type of lithological unit is transformed in a probability of occurrence using statistical methods, but alternatively can also be expressed as a fuzzy membership for the expected occurrence of landslides using subjective judgment or/and objective analysis based on fuzzy logic.

Zimmerman (1996) discussed a variety of combination rules for fuzzy membership functions. An et al. (1991) and Bonham-Carter (1994) discussed five operators that can be used to combine fuzzy membership functions related to landslide causative factors, namely the fuzzy AND, fuzzy OR, fuzzy algebraic product, fuzzy algebraic sum and fuzzy gamma operator. In the present study, all five fuzzy operators are tested to determine the most successful method for landslide susceptibility mapping.

Fuzzy Operators

The fuzzy AND operator is equivalent to a Boolean AND (logical intersection), defined as:

$$\mu_{combination} = \min (\mu_A, \mu_B, \mu_C, ...), \qquad (1)$$

where $\mu_{combination}$ is the combined fuzzy membership function, μ_A is the membership value for map A at a particular location, μ_B is the value for map B, etc.

The fuzzy OR is equivalent to the Boolean OR (logical union), defined as:

$$\mu_{combination} = \max (\mu_A, \mu_B, \mu_C, ...). \qquad (2)$$

The fuzzy algebraic product is defined as:

$$\mu_{combination} = \prod_{i=1}^{n} \mu_i , \qquad (3)$$

where μ_i is the fuzzy membership function of the ith map and i = 1,2,...,n maps are to be combined.

The fuzzy algebraic sum is complementary to the fuzzy algebraic product and defined as:

$$\mu_{combination} = 1 - \prod_{i=1}^{n}(1 - \mu_i) \qquad (4)$$

The fuzzy gamma operation is defined in terms of the fuzzy algebraic product and the fuzzy algebraic sum as:

$$\mu_{combination} = [\prod_{i=1}^{n}\mu_i]^{\gamma}[1 - \prod_{i=1}^{n}(1 - \mu_i)]^{1-\gamma} \quad (5)$$

where γ is a parameter chosen in the range [0,1]; when γ is 1 the operator is equivalent to the fuzzy algebraic product and when γ is 0 it is equivalent to the fuzzy algebraic sum.

Assignment of Fuzzy Membership Values

Different methodologies have been proposed in the literature to assign fuzzy membership values, such as normalization between zero and one of rating values given by expert and field knowledge (Tangestani, 2004; Champati ray et al., 2007), normalization of frequency ratio values (Lee, 2007; Pradhan et al., 2009; Regmi et al., 2010), fuzzy conditional statement (Ercanoglu and Gokceoglu, 2002), or the cosine amplitude method (Ercanoglu and Gokceoglu, 2004; Kanungo et al., 2006; Gupta et al., 2008; Kanungo et al., 2009). In this study, fuzzy membership values for each causative factor were obtained by normalization of the likelihood ratios as shown in Table 2. The likelihood ratio is defined as:

$$W_{ij} = f_{ij} / f = (A_{ij}^* / A^*) (A/A_{ij}), \qquad (6)$$

where W_{ij} is the weight or likelihood ratio of a certain class i of parameter j, f_{ij} the landslide density within class i of parameter j, f the landslide density within the entire map, A_{ij}^* the area of landslides in class i of parameter j, A_{ij} the area of class i of parameter j, A^* the total area of landslides in the entire map, and A the total area of the entire map. If the likelihood ratio is greater than 1, the relationship between landslides and the factors is high and, if the ratio is less than 1, the relationship between landslide and the factors is lower. After normalization of the likelihood values, fuzzy membership values were obtained as shown in the last column of Table 2 and given as

$$\mu_{ij} = W_{ij} / max_i (W_{ij}), \qquad (7)$$

where μ_{ij} is the fuzzy membership value of class i of parameter j.

APPLICATION OF FUZZY LOGIC TO LANDSLIDE SUSCEPTIBILITY MAPPING

The seven causative factors (slope aspect, slope angle, soil rock type, distance from drainage, geology, land cover and distance from faults and folds) were combined to produce a landslide susceptibility index map using the fuzzy operators AND, OR, algebraic product, algebraic sum and the gamma operator. For the fuzzy gamma operator different values for γ from 0.1 to 0.9 with steps of 0.1 were applied. The results are shown in Fig.7. Figure 7a depicts the cumulative percentage of observed landslide occurrence versus the obtained combined fuzzy membership function $\mu_{combination}$. For the gamma operator only results for γ equal to 0.1, 0.6 and 0.9 are shown in order not to overcrowd the graph. One can clearly notice the effects of the different fuzzy operators. The AND, OR and algebraic sum operators produce very crisp results. Moreover, the combined fuzzy membership values for the algebraic sum operator are very extreme, i.e. between 0.9 and 1. Also, the combined fuzzy membership values for the fuzzy OR operator are rather high. On the other hand, the algebraic product and gamma operators produce much more evenly distributed fuzzy membership values, although the values are rather skewed to the lower end for the algebraic sum and gamma operator with γ equal to 0.1. The results for the gamma operator with γ equal to 0.6 and 0.9 clearly produce the most evenly distributed combined fuzzy membership values.

To compare quantitatively the results obtained with the different fuzzy operators, success rate curves (Chung and Fabbri, 1999; van Westen et al., 2003) are shown in Fig.7b for each fuzzy operator. To obtain a success rate curve, the cumulative percentage of observed landslide occurrence is plotted against the cumulative areal percentage of decreasing $\mu_{combination}$ values (Fig.7b). The area under the curve expresses the overall success rate, i.e. how well the combined fuzzy membership values predict the observed landslides. The resulting values for the different fuzzy operators are given in Table 3 expressed in percentages. For instance, for the fuzzy AND operator the area under the curve 0.7144, which implies that the overall success rate accuracy is 71.44%. Table 3 shows that the fuzzy sum operator has the lowest success rate accuracy among the 13 different cases, followed by the fuzzy OR operator. Hence, these operators are not very suited for landslide susceptibility mapping. The fuzzy AND operator produces fair intermediate results, i.e. 71.44%. But, the fuzzy product and gamma operators clearly produce the best, almost identical results for the success rate accuracy, i.e. between 79.29 to 80.11%. The very best

Success rate accuracy for the different fuzzy operators

Fuzzy operator	Success rate(%)
AND	71.44
OR	64.01
Algebraic sum	50.92
Algebraic product	79.29
Gamma operation	
$\gamma = 0.1$	79.73
$\gamma = 0.2$	79.84
$\gamma = 0.3$	79.98
$\gamma = 0.4$	80.08
$\gamma = 0.5$	80.05
$\gamma = 0.6$	80.11
$\gamma = 0.7$	80.08
$\gamma = 0.8$	80.04
$\gamma = 0.9$	80.02

area has moderate values, 20% has high values and the remaining 10% of the study area has the highest values. In order to physically validate the landslide susceptibility map, the landslide susceptibility zones displayed on the map can be compared and verified with field information on past landslides, especially for the high and very high susceptible zones. In the present case, it is observed that large landslides such as debris slides, rockslides, plane failure, etc. are clearly marked in the areas of high and very high susceptible zones. Quantitative comparison with the observed landslide inventory, shows that the very high susceptible zone contains 41.31% of the total observed landslide occurrences, whereas, the high, moderate and low susceptible zones cover 32.02%, 22.22% and 4.45%, respectively (Fig.8, Table 4). The overall quality of the landslide susceptibility map can also be assessed by the landslide density of each class (Sarkar and Kanungo, 2004). The results are given in the last column of Table 4. From the table, it can be observed that the landslide density for the very high susceptible zone is 0.0605, which is distinctly higher than for the other susceptible zones and almost five times larger than the overall landslide density of 0.0146. Furthermore, there is a gradual decrease in density values from very high to low susceptible zone and there is also considerable separation in landslide density values between the susceptible zones. Hence, it can be inferred that the

Fig.7. Graphs showing results obtained with the different fuzzy operators: (**a**) cumulative percentage of observed landslide occurrences versus combined fuzzy membership function, (**b**) success rate curves, i.e. cumulative percentage of observed landslide occurrences versus cumulative areal percentage of decreasing combined fuzzy membership values.

success rate accuracy of 80.11% is obtained with the fuzzy gamma operator for γ equal to 0.6. This fuzzy operator also produces very evenly distributed combined fuzzy membership values, which very likely explains its success in predicting the observed landslide locations.

Consequently, the combined fuzzy membership map obtained with the fuzzy gamma operator for $\gamma = 0.6$ was selected to derive the landslide susceptibility map (Fig.8). This map is categorized into low, moderate, high and very high landslide susceptible zones such that 40% of the study area has low fuzzy membership values, 30% of the study

Table 4. Areal distribution of susceptible zones and observed landslides, and resulting landslide density

Susceptible zones	Area		Landslide		Landslide density
	(km²)	(%)	(km²)	(%)	
Low	56.53	40.00	0.09	4.45	0.0016
Moderate	42.40	30.00	0.46	22.22	0.0108
High	28.27	20.00	0.66	32.02	0.0234
Very high	14.13	10.00	0.85	41.31	0.0605
Total	**141.33**	**100.00**	**2.07**	**100.00**	**0.0146**
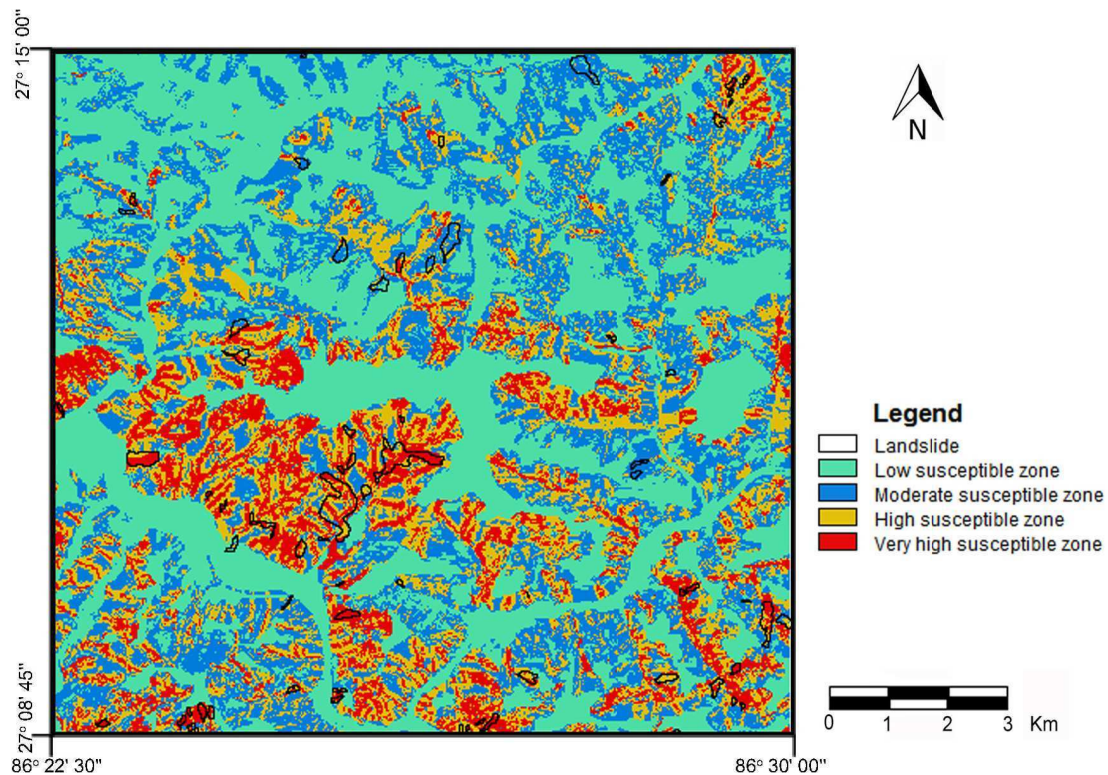
Fig.8. Landslide susceptibility map derived from the combined fuzzy membership function results obtained with the fuzzy gamma operator for γ = 0.60.

landslide susceptible zones reflect the existing slope instability conditions observed in the field.

CONCLUSION

The fuzzy logic approach is one of the easiest and simplest methods to prepare a landslide susceptibility map. Different fuzzy operators and different γ values for the fuzzy gamma operation can be used to prepare landslide susceptibility maps. On the basis of success rate curves, the fuzzy operator producing the best success rate accuracy can be identified and used to generate the most reliable landslide susceptibility zonation map. In the present study, seven causative factors (slope aspect, slope angle, soil rock type, distance from drainage, geology, land cover and distance from faults and folds) were combined using five different fuzzy operators. The landslide susceptibility index maps produced by the fuzzy product and fuzzy gamma operator with different γ values reveal an almost similar success rate accuracy, i.e. about 80%. On the other hand, the fuzzy OR and fuzzy sum operators generate much worse results as the accuracy of the success rates is only about 50-60%, while the fuzzy AND operator performance is intermediate. As the fuzzy gamma operator with a γ value of 0.60 produces

the best success rate accuracy, the final landslide susceptibility zonation map is derived with this operator. The very high susceptible zone on this map covers 10% of the study area and predicts 41.4% of the past landslides, while the high susceptible zone covers 20% of the study area and predicts 32.0% of the past landslides. These are encouraging results for a first attempt to understand landslide phenomena in this area.

During infrastructure development works, care should be taken to avoid the very high and high landslide susceptible zones. Roads, buildings, irrigation canal, etc. should be constructed in the moderate and low susceptible zones. In case of existing infrastructures that lie in the high susceptible zone, slope stability works should be performed for the protection of these structures. For the Harkapur–Okhaldhunga road section passing through the high susceptible zone in the Bhadare Khola and in north of Hilepani, slope stability measure should be carried out to protect the road from further deterioration. The landslide susceptibility map can also be used in disaster management planning such as the preparation of rescue routes, service centres and shelters.

Very likely, the landslide susceptibility analysis would be even more accurate if rainfall had also been considered

as a causative factor. But unfortunately, rainfall stations and observation data in and around this area are lacking. If representative data of rainfall in the area are obtained, it would be worthwhile to redo the analysis to obtain better results.

References

ACHARYA, G., DE SMEDT, F. and LONG, N. T. (2006) Assessing landslide hazard in GIS: a case study from Rasuwa, Nepal. Bull. Engg. Geol. Environ., v.65(1), pp.99–107.

ACHARYA, K.K. (2008) Qualitative kinematic investigations related to the extrusion of the Higher Himalayan Crystalline and equivalent tectonometamorphic wedges in the central Nepal Himalaya. PhD thesis, Universitat Wien, Austria.

ALEOTTI, P. and CHOWDHURY, R. (1999) Landslide hazard assessment: summary review and new perspectives. Bull. Engg. Geol. Environ., v.58(1), pp.21–44.

AN, P., MOON, W.M. and RENCZ, A. (1991) Application of fuzzy set theory to integrated mineral exploration. Canadian Jour. Explor. Geophys., v.27(1), pp.1–11.

BONHAM-CARTER, G.F. (1994) Geographic information systems for geoscientists, modelling with GIS. Pergamon, Oxford, 398p.

CHAMPATI RAY, P.K., DIMRI, S., LAKHERA, R.C. and SATI, S. (2007) Fuzzy-based method for landslide hazard assessment in active seismic zone of Himalaya. Landslides, v.4, pp.101–111.

BIJUKCHHEN, S.M., KAYASTHA, P. and DHITAL, M.R. (2012) A comparative evaluation of heuristic and bivariate statistical modelling for landslide susceptibility mappings in Ghurmi-Dhad Khola, east Nepal. Arab Jour. Geosci. (doi: 10.1007/s12517-012-0569-7)

CHUNG, C.F. and FABBRI, A.G. (1999) Probabilistic prediction models for landslide hazard mapping. Photogrammetric Engg. Remote Sensing, v.65(12), pp.1389"1399.

DAHAL, R.K., HASEGAWA, S., NONOMURA, A., YAMANAKA, M., DHAKAL, S. and PAUDYAL, P. (2008) Predictive modelling of rainfall-induced landslide hazard in the Lesser Himalaya of Nepal based on weights-of-evidence. Geomorphology, v.102, pp.496–510.

DEOJA, B.B., DHITAL, M. R., THAPA, B. and WAGNER, A. (1991) Mountain risk engineering handbook. International Centre for Integrated Mountain Development (ICIMOD), Kathmandu, Nepal,875p.

DHAKAL, A. S., AMADA, T. and ANIYA, M. (1999) Landslide hazard mapping and the application of GIS in the Kulekhani watershed Nepal. Mountain Research and Development, v.19(1), pp.3–16.

DHITAL, M.R. (2005a) Landslide investigation and mitigation in Himalayas: focus on Nepal. Proc. International Symposium "Landslide Hazard in Orogenic Zone from the Himalaya to Island Arc in Asia", Kathmandu, Nepal, pp.1-15.

DHITAL, M.R. (2005b) Study of damage caused by rainfall in Hilepani-Jayaramghat-Diktel environment friendly road. Report submitted to the Rural Access Programme (RAP), Kathmandu, Nepal.

DUBEY, C.S., CHAUDHRY, M., SHARMA, B.K., PANDEY, A.C. and SINGH, B. (2005) Visualization of 3-D digital elevation model for landslide assessment and prediction in mountainous terrain: A case study of Chandmari landslide, Sikkim, eastern Himalayas. Geosciences Jour., v.9(4), pp.363–373.

ERCANOGLU, M. and GOKCEOGLU, C. (2002) Assessment of landslide susceptibility for a landslide-prone area (north of Yenice, NW Turkye) by fuzzy approach. Environ. Geol., v.41, pp.720–730.

ERCANOGLU, M. and GOKCEOGLU, C. (2004) Use of fuzzy relations to produce landslide susceptibility map of a landslide prone area (West Black Sea Region, Turkey). Engg. Geol., v.75, pp.229–250.

GHIMIRE, M. (2011) Landslide occurrence and its relation with terrain factors in the Siwalik Hills, Nepal: case study of susceptibility assessment in three basins. Natural Hazards, v.56, pp.299–320.

GOSCOMBE, B., GRAY, D. and HAND, M. (2006) Crustal architecture of the Himalayan metamorphic front in eastern Nepal. Gondwana Res., v.10, pp.232–255.

GUPTA, R.P., KANUNGO, D.P., ARORA, M.K. and SARKAR, S. (2008) Approaches for comparative evaluation of raster GIS-based landslide susceptibility zonation maps. International Jour. Appld. Earth Observation and Geoinformation, v.10, pp.330–341.

GUZZETTI F., CARRARA, A., CARDINALI, M. and REICHENBACH, P. (1999) Landslide hazard evaluation: a review of current techniques and their application in a multi-scale study, Central Italy. Geomorphology, v.31, pp.181–216.

GYAWALI, B. and BIJUKCHHEN, S.M. (2011) Geological map of the Ghurmi-Dhad Khola area, Eastern Nepal (Scale 1:25,000). Central Department of Geology, Tribhuvan University, Kathmandu, Nepal.

ISHIDA, T. and OHTA, Y. (1973) Ramechhap-Okhaldunga region. In: S. Hashimoto, Y. Ohta, and C. Akiba, C. (Eds.), Geology of the Nepal Himalayas. Saikon, Sapporo (Japan), pp.35–68.

JOSHI, J., MAJTAN, S., MORITA, K. and OMURA, H. (2000) Landslide hazard mapping in the Nallu Khola watershed, Central Nepal. Jour. Nepal Geol. Soc., v.21, pp.21–28.

KANUNGO, D. P., ARORA, M. K., GUPTA, R.P. and SARKAR, S. (2008) Landslide risk assessment using concepts of danger pixels and fuzzy set theory in Darjeeling Himalayas. Landslides, v.5, pp.407–416.

KANUNGO, D.P., ARORA, M.K., SARKAR, S. and GUPTA, R.P. (2006) A comparative study of conventional, ANN black box, fuzzy and combined neural and fuzzy weighting procedures for landslide susceptibility zonation in Darjeeling Himalayas. Engg. Geol., v.85, pp.347–366.

KANUNGO, D.P., ARORA, M.K., SARKAR, S. and GUPTA, R.P. (2009) A fuzzy set based approach for integration of thematic maps for landslide susceptibility zonation. Georisk: Assessment and Management of Risk for Engineered Systems and Geohazards, v.3(1): pp.30–43.

KAYASTHA, P. and DE SMEDT, F. (2009) Regional slope instability zonation using GIS technique in Dhading, Central Nepal. In: J.P. Malet, A. Remaître and T. Boggard. (Eds.), Landslide Processes: From Geomorphologic Mapping to Dynamic Modelling, CERG, France, pp.303–309.

KAYASTHA, P., DE SMEDT, F. and DHITAL, M.R. (2010) GIS based landslide susceptibility assessment in Nepal Himalaya: a comparison of heuristic and statistical bivariate analysis. In: J.P. Malet, T. Glade and N. Casagli (Eds.), Mountain Risks: Bringing Science to Society, CERG Editions, France, pp.121–128.

KAYASTHA, P., DHITAL, M.R. and DE SMEDT, F. (2012) Landslide susceptibility mapping using the weight of evidence method in the Tinau watershed, Nepal. Natural Hazards (doi: 10.1007/s11069-012-0163-z)

LEE, S. (2007) Application and verification of fuzzy algebraic operators to landslide susceptibility mapping. Environ. Geol., v.52, pp.615–623.

LEE S., SONG, K-Y., OH H-J. and CHOI, J. (2012) Detection of landslides using web-based aerial photographs and landslide susceptibility mapping using geospatial analysis. International Jour. Remote Sensing, v.33(16), pp.4937–4966.

LONG, N.T. (2008) Landslide susceptibility mapping of the mountainous area in A Luoi District, Thua Thein Hue Province, Vietnam. PhD thesis in Engineering, Vrije Universiteit Brussel, Belgium. 229 pp.

NADIM, F., KJEKSTAD, O., DOMAAS, U., RAFAT, R. and PEDUZZI, P. (2006) Global Landslides Risk Case Study. In: M. Arnold, R.S. Chen, U. Deichmann, M. Dilley, A.L. Lerner-Lam, R.E. Pullen, and Z. Trohanis (Eds.), Natural Disaster Hotspots, Case Studies. Disaster Risk Management Series No. 6. The World Bank, Hazard Management Unit, Washington DC, USA, pp.21–77.

PANTHA, B. R., YATABE, R. and BHANDARY, N.P. (2010) GIS-based highway maintenance prioritization model: an integrated approach for highway maintenance in Nepal mountains. Jour. Transport Geography, v.18, pp.426–433.

POUDYAL, C. P., CHANG, C., OH, H. and LEE, S. (2010) Landslide susceptibility maps comparing frequency ratio and artificial neural networks: a case study from the Nepal Himalaya. Environ. Earth Sci, v.61, pp.1049–1064.

PRADHAN, B., LEE, S. and BUCHROITHNER, M. F. (2009) Use of geospatial data and fuzzy algebraic operators to landslide-hazard mapping. Applied Geomatics, v.1, pp.3–15.

RAY, R.L. and DE SMEDT, F. (2009) Slope stability analysis on a regional scale using GIS: a case study from Dhading, Nepal. Environ. Geol., v.57, pp.1603–1611.

REGMI, N.R. GIARDINO, J.R. and VITEK, J.D. (2010) Assessing susceptibility to landslides: Using models to understand observed changes in slopes. Geomorphology, v.122, pp.25–38.

SARKAR, S. and KANUNGO, D.P. (2004) An integrated approach for landslide susceptibility mapping using remote sensing and GIS. Photogrammetric Engineering and Remote Sensing, v.70(5), pp.617–625.

SHARMA, R.H. and SHAKYA, N.M. (2008) Rain induced shallow landslide hazard assessment for ungauged catchments. Hydrogeology Jour., v.16, pp.871–877.

TANGESTANI, M.H. (2004) Landslide susceptibility mapping using the fuzzy gamma approach in a GIS, Kakan catchment area, southwest Iran. Australian Jour. Earth Sci., v.51(3), pp.439–450.

SINGH, R.P., DUBEY, C.S., SINGH, S.K., SHUKLA, D.P., MISHRA, B.K., TAJBAKHSH, M., NINGTHOUJAM, P.S., SHARMA, M. and SINGH, N. (2012) A new slope mass rating in mountainous terrain, Jammu and Kashmir Himalayas: application of geophysical technique in slope stability studies. Landslides. (doi: 10.1007/s10346-012-0323-y)

THAPA, P.B. and DHITAL, M.R. (2000) Landslide and debris flows of 19–21 July 1993 in the Agra Khola watershed of central Nepal. Jour. Nepal Geol. Soc., v.21, pp.5–20.

UPRETI, B.N. and DHITAL, M.R. (1996) Landslide studies and management in Nepal. International Centre for Integrated Mountain Development (ICIMOD), Kathmandu, Nepal, 87p.

VAN WESTEN, C.J., RENGERS, N. and SOETERS, R. (2003) Use of geomorphological information in indirect landslide susceptibility assessment. Natural Hazards, v.30, pp.399–419.

ZADEH, L.A. (1965) Fuzzy sets. Information and Control. v.8, pp.338–353.

ZIMMERMAN, H.J. (1996) Fuzzy set theory and it applications. Kluwer Academic Publishers, Norwell MA, USA. 435p.